Pergamon

Spectrochimica Acta, Vol. 50B, Nos. 4–7, pp. 583–605, 1995

0584–8547/95 $9.50 + .00

0584–8547(94)00158–8

Experimental determination of the energy distribution of ions bombarding the cathode surface in a glow discharge*

MARK VAN STRAATEN, ANNEMIE BOGAERTS and RENAAT GIJBELS†
University of Antwerp (UIA), Department of Chemistry, Universiteitsplein 1, B-2610 Wilrijk-Antwerp, Belgium

(*Received* 15 *June* 1994; *accepted* 8 *September* 1994)

Abstract—The energy distribution of ions bombarding the cathode in a glow discharge is measured. Reproducible results are obtained for X^+, X^{2+}, X_2^+, M^+ and MX^+ ion species where X denotes the gas used (argon and neon) and M the cathode material (Al, Cu, Mo and Ta), and illustrate that the cathode is bombarded by low energy singly charged gas ions and by a significant flux of high energy singly charged ions of its own material. Singly charged gas ion motion in the cathode dark space is largely dominated by charge exchange collisions; cathode ions reach the cathode with an energy almost equal to the full discharge potential equivalent due to the low probability of asymmetrical charge exchange. The number of charge exchange collisions with neutral gas atoms, either symmetrical or asymmetrical, determines the energy distribution of all kinds of ions at the cathode and is influenced by the mean free path and the length of the dark space. The variation of the discharge parameters shows that the ratio of these both quantities is not necessarily constant, at least for a glow discharge operating at conditions typical for analytical mass spectrometry (10–100 Pa, 1–5 mA, 500–1500 V).

1. INTRODUCTION

GLOW discharges are becoming widely accepted as primary sources for atomic spectrometry. Both optical emission and mass spectrometers are coupled with glow discharge sources, and allow the direct analysis of solid samples without the need for a dissolution step [1, 2]. This can, among other things, offer a considerable time advantage and minimize contamination problems. Whereas with conventional dc GD sources one is restricted to conducting samples (or non-conducting samples mixed with a conducting host matrix), it has been shown that rf GDs can be applied which also extend the applicability of these devices to non-conducting matrices [3].

The GD used in atomic spectrometry has a double function: it serves both as a means of sample atomization and it creates the necessary analytical signal of the atoms. The latter is measured by a certain spectrometric technique (e.g. optical emission or mass spectrometry), and is directly related to the sample composition. The strength of a GD lies in the fact that although it provides for both functions, the atomization step and subsequent formation of the analytical signal are separated in time and space and are, equally importantly, relatively non-selective processes. The atomization of sample material is achieved by sputtering, mostly by gas ions and fast gas atoms, and the sputtered atoms diffuse to another part of the discharge environment (the negative glow) where collisions with other particles (mainly electrons and excited gas atoms) take care of the excitation or ionization.

It is clear that no special sample introduction systems exist for GD sources, because the sample itself forms part of the discharge by serving as the cathode of the system. However, strictly speaking, one can regard the intrinsic sputter atomization step and the subsequent diffusion of sputtered material into the negative glow region as a method of "sample introduction" and it goes without saying that the processes involved are crucial for the implementation of a GD as a spectrometric source. Diffusion of

* This paper was published in the Special Issue on Sample Introduction in Atomic Spectrometry.
† To whom correspondence should be addressed.

sputtered material has been studied by several authors [4–6], both theoretically and experimentally. Detailed information on the sputtering process is, however, somewhat more scarce, i.e. exactly which particles bring about the sputtering and what is the energy with which they reach the cathode (sample) surface? The work of DAVIS and VANDERSLICE [7] can be regarded as the "reference" on this topic. They used a double focusing mass spectrometer of forward geometry to determine the energy distribution of ions striking the cathode of a GD in hydrogen, helium, neon and argon. Although it dates back to the early 1960s, not many data have been reported since by other authors, which is perhaps mostly due to the experimental difficulties accompanying the determination of a "true" energy distribution free of instrumental artifacts. Papers by BONDARENKO and co-worker [8, 9] describe comparable results for discharges in air, nitrogen, oxygen, argon and helium. They were the first to mention that ions of the cathode material also bombard the cathode surface (for a helium discharge). Another interesting and related work by DENK [10] deals with the mass spectrometric detection of ions and their energy distributions at the cathode of GDs in argon and nitrogen, and confirms to a large extent the results obtained by DAVIS and VANDERSLICE [7].

Considering the somewhat scarce literature data, it seemed worthwhile performing similar experiments to those described by DAVIS and VANDERSLICE [7], under typical analytical discharge conditions. It is obvious that the energy of gas ions which bombard the cathode will be determined by the collisons (predominantly charge exchange collisions) in which they participate during their acceleration across the dark space. By the application of theoretical models; we are able to calculate the gas ion energy distribution at the cathode surface of a GD [11–13] and the first aim was to investigate whether analogous energy distributions to those theoretically predicted could also be measured, including the effect of parameter changes (discharge conditions) on these distributions. Also the relevance of self-sputtering, i.e. bombardment of the cathode with ions of its own material, is evaluated, which was not incorporated in any of the previous investigations.

Several methods exist to measure the energy distribution of ions which underwent a certain formation process, dependent on the available instrumentation. Mass spectrometry offers a considerable advantage: ions of different mass can be separated so that the energy distribution of different ions can be determined. Only information about the ions can be acquired; it is not possible to directly measure the energy distribution of the neutrals impinging on the surface without post-ionization, such as electron impact ionization.

2. THEORETICALLY EXPECTED GAS ION ENERGY DISTRIBUTION AT THE CATHODE

The basic operating properties of a GD can be represented schematically by Fig. 1, incorporating for simplicity only the cathode dark space (CDS) and negative glow (NG) as discharge zones. These are also the two zones of analytical importance: the sputter atomization step is determined by the processes occurring in the cathode dark space, whereas the NG region is important for the excitation and/or ionization of sputtered material. Only excitation and ionization are taken into account as the only possible inelastic collision processes for electrons with gas atoms. In this figure, (directional) motion of charged species under the influence of the electric field, assumed only to exist in the dark space, is represented by thick lines, whereas diffusion, i.e. random motion, is represented by thin lines.

The existence of some electron population in the CDS close to the cathode is taken as the starting point. This electron population is accelerated in the CDS and forms a beam of fast electrons which would enter the NG with an energy corresponding to the full discharge potential and finally hit the anode if no inelastic collisions were to occur. However, excitation and ionization of gas atoms in both regions allow the electrons to lose some of their energy. If this takes place in the CDS, the slowed down primary and newly created secondary electrons (in the case of ionization) are

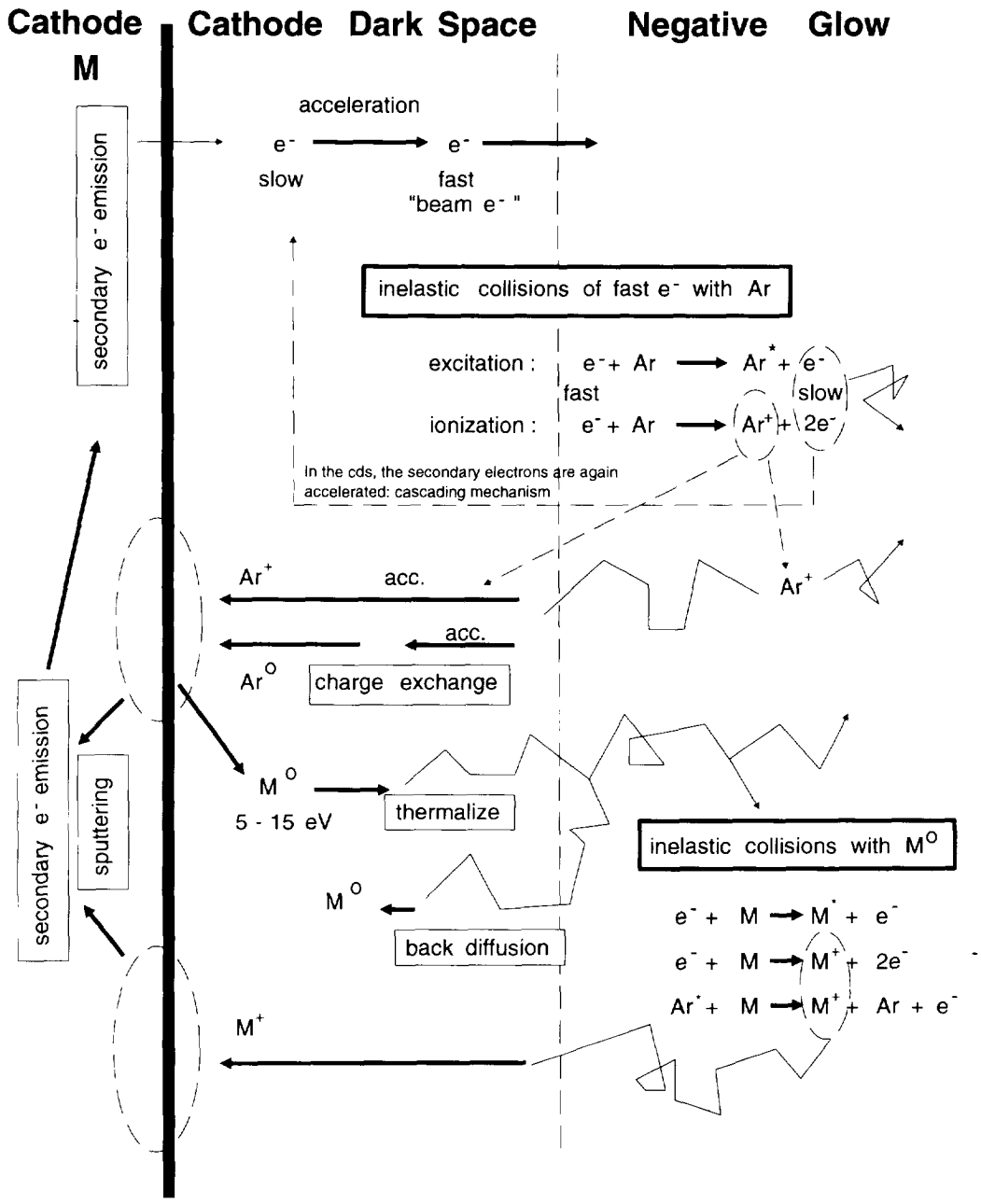

Fig. 1. Schematic representation of the basic processes occurring in a glow discharge (anode phenomena are not included).

again accelerated, giving a cascade mechanism of electron production. In the NG, slowing down by inelastic collisons forms a large population of low energy electrons whose motion will finally be diffusion controlled if they are completely thermalized.

Gas ions created by electron impact ionization in the CDS are directly under the influence of the electric field and accelerated towards the cathode surface. Ions formed in the NG can reach the NG/CDS interface by diffusion and also contribute to the ion current to the cathode. When accelerated, these ions are likely to produce fast atoms by charge exchange collisions. Symmetrical charge exchange is a resonance process of high probability. When the gas ion transfers its charge to the gas atom, it keeps its energy and no energy is consumed. This indicates that the cathode is bombarded by large fluxes of ions and fast gas atoms. Upon impact, they result in

the input of new electrons to the system through secondary electron emission and the circle is complete.

Besides secondary electron emission, ion and atom bombardment will also cause sputtering of cathode material. Here it is assumed that these sputtered atoms lose their initial energy of a few electronvolts through collisions in the gas environment, whereafter they diffuse further into the NG or back to the sample surface. In the NG, inelastic collisions of the sample atoms with either electrons or metastable gas atoms result in excitation or ionization of sample material. Ionized sample atoms may eventually diffuse back towards the CDS and come under the influence of the electric field, also causing sputtering and secondary electron emission when hitting the surface.

Based on the solution of a set of coupled differential equations (Boltzmann equations) describing the transport of gas species (ions and fast atoms) and electrons in the CDS, or on the solution of a Monte Carlo scheme [11–13], it is possible to calculate the effect of the two collision processes (electron impact ionization and charge transfer) on the energy of the particles hitting the cathode surface. These model calculations show, among other things, that symmetrical charge exchange is a process of considerable importance: it reduces the average energy of the gas ions at the cathode to only a fraction of the maximum attainable energy given by the discharge voltage and creates a large neutral atom flux which also bombards the cathode. Sputtering in a glow discharge is thus, at least theoretically, the combined effect of ion and fast neutral bombardment. For a 1000 V argon discharge with a molybdenum cathode, the flux energy distributions of argon ions and fast neutrals at the cathode surface (i.e. the number of particles bombarding the cathode per cm^2 and per second as a function of energy) are presented in Fig. 2 for three different pressure regimes (and hence also three different current densities for a GD operating in the abnormal mode [14]). The x axis is a relative energy axis, giving the fraction of the maximum attainable energy $E_{max} = eV_{disch}$. It can be seen that the x axis is truncated for both the ion and neutral distributions, but at different values of E/E_{max}. At higher pressures the total flux of bombarding species increases because higher pressures yield higher discharge currents at constant voltage.

To theoretically evaluate the effect of the pressure more closely, the influence of the discharge current can be ruled out by normalizing the flux distributions to the total area under the curves shown in Fig. 2. The result is presented in Fig. 3(a) for the ions. The three normalized distributions now almost coincide and the expected shift to lower energies at a higher pressure (because of the increased collision probability at higher pressure) is not visible. Here it has also, however, to be remembered that the length of the dark space d_c, decreases with increasing pressure [12, 15]. Hence it is not the mean free path for charge exchange (being the most important energy loss process for the gas ions) l_{cc}, which determines the outlook of the distributions, but rather the ratio d_c/l_{cc}. The fact that no clear difference in ion energy distributions is obtained for different pressures indicates that, at least theoretically, this ratio is nearly constant, giving an almost constant number of collisions throughout the dark space and thus comparable energy distributions. Examining the normalized flux distributions of ions (at the cathode) for a constant pressure (50 Pa) but different discharge voltages (or currents) yields an extra confirmation (Fig. 3(b)). At constant pressure, the effect of the discharge voltage on the charge exchange collisions will be minor because l_{cc} does not vary much with the energy of the colliding ion. The efficiency of electron impact ionization, however, drops with increasing energy of the electrons. Hence, for a higher discharge voltage, a lower electric field will ensure the maintenance of a certain current density, giving a shorter dark space distance. At lower voltages, the variation of the dark space length is more pronounced than at higher voltages reflecting the larger variation in ionization efficiency at lower voltages compared to higher voltages. This effect of the discharge voltage at constant pressure on the dark space length is indeed also noticeable in the energy distributions of the gas ions at the cathode given in Fig. 3(b). The energy distributions are now completely governed by the length of the dark space d_c;

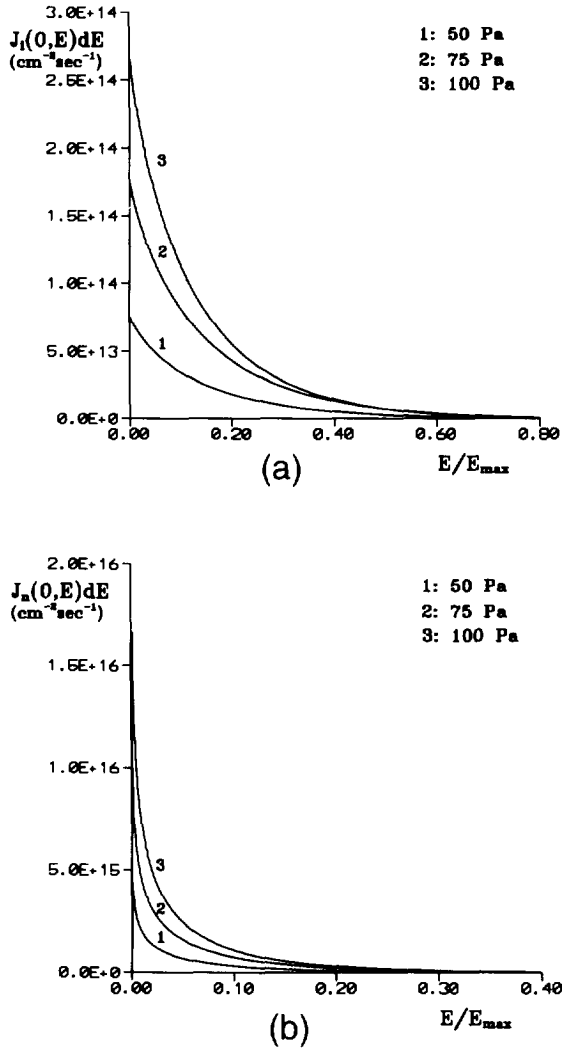

Fig. 2. Calculated flux energy distributions for argon ions (a) and fast neutrals (b) at the cathode surface for a 1000 V discharge at three pressures (Mo/Ar system).

the ratio d_c/l_{ce} is more different for the three discharge conditions and this is reflected in the normalized distributions. A shift to lower ion energies is observed for lower discharge voltages, attributable to an increase in dark space length and thus to a larger number of charge exchange collisions.

3. Experimental

All experiments were peformed using a VG9000 glow discharge mass spectrometer, a double focusing instrument of reversed Nier–Johnson goemetry with the magnetic sector placed in front of the electrostatic sector. In order to sample a representative population of ions hitting the cathode in a GD and then to determine the energy distribution of each ionic species with as little energy discrimination as possible, several modifications to the instrument had to be carried out. Firstly, in normal analytical conditions ions are sampled out of the negative glow region of the GD, the wrong part of the plasma for the present investigation. Secondly, the typical measurement sequence in normal operation yields a mass spectrum, not an energy spectrum, and does not care much about avoiding energy discrimination. On the contrary, a specially designed lens system is applied to maximize beam intensity and/or mass resolution which intrinsically can mean energy focusing or defocusing.

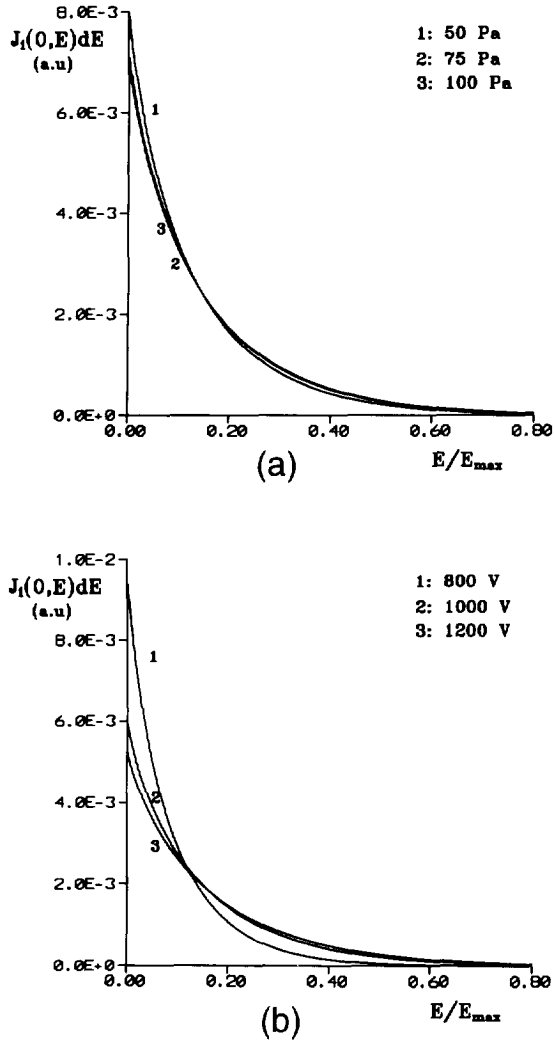

Fig. 3. Normalized calculated flux energy distributions for argon ions at the cathode surface: (a) for a 1000 V discharge at three different pressures; (b) for three different voltages at a pressure of 50 Pa.

3.1. *Accelerating voltage scan*

One approach in mass spectrometric ion energy analysis is based on the variation of the acceleration voltage given to the ions to traverse the mass spectrometer. Consider a double focusing mass spectrometer coupled with a certain ion source which, after optimization, yields a certain intensity measured by the detector for ions of a given mass. This means that the instrument (accelerating voltage, magnetic field strength and electrostatic sector voltage) is tuned in such a manner that ions with a specific total kinetic energy (and of course also of a specific mass-to-charge ratio) are able to reach the detector. Now, when the magnetic field and the electrostatic sector voltage are kept constant, ions with this specific mass but with another energy can also be transmitted if the accelerating voltage is altered. A numerical example can clarify this. A mass spectrometer is adjusted to detect ions of atomic mass 40 and a total energy of 5 keV. Suppose that the ion formation process yields single charged ions with an initial energy of 100 and 200 eV (hypothetically). To obtain transmission of the 100 eV ions, the accelerating voltage should be set to a vlaue of 4.9 kV and for the 200 eV ions this becomes 4.8 kV, because then in both cases their total energies amount to 5 keV. A necessary condition is, however, that magnetic and electrostatic field strengths are kept constant. For the detection of a more continuous

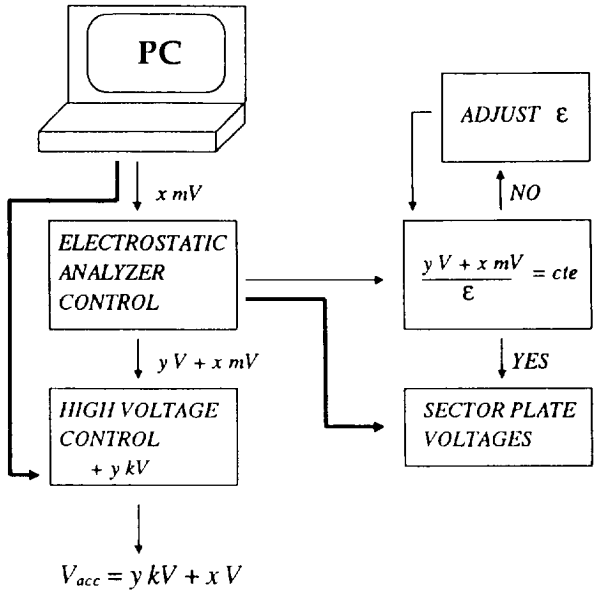

Fig. 4. Measurement strategy for normal mass scanning (thin lines) and kinetic energy scanning (thick lines) for the VG9000 mass spectrometer.

initial energy distribution, the accelerating voltage can be varied between certain limits.

The main difficulty which arises for the mass spectrometric determination of an energy distribution is avoiding any possible energy discrimination when the ion beam traverses the mass spectrometer. For every part of the instrument, the preferential focusing of ions with a certain energy has to be ruled out or minimized. Preferential focusing can be caused mainly by beam defining slits and/or by electrostatic lens systems. Beam defining slits can induce energy discrimination when the ion beam is not spatially homogeneous in energy and thus can filter out ions of a certain energy.

The total voltage drop in a GD, typically between 500 and 1500 V in analytical applications, is situated in the CDS just in front of the cathode. This means that singly charged ions arriving at the cathode can have energies ranging from virtually 0 eV for ions formed very close to the cathode surface, to an energy equivalent to full discharge potential corresponding to ions accelerated across the whole dark space without taking part in any collision event. To acquire an energy spectrum, all these ions must be allowed to pass through the mass spectrometer by applying an appropriate accelerating voltage at constant electrostatic sector voltage and a magnetic field setting for a certain mass.

In normal analytical configuration of the VG9000 instrument, peak scanning (mass scanning) is performed by varying the accelerating voltage and the electrostatic sector voltage whilst keeping their ratio constant. For the present purpose both have to be decoupled so that the accelerating voltage can be changed independently. By a suitable modification in the control of the mass spectrometer this could be achieved while at the same time the scanning capabilities of the instrument via the computer could be maintained, but in a much larger voltage range. The essence of the method is to superimpose a sawtooth shaped voltage on a constant potential of a few kilovolts using their sum as the accelerating voltage.

The measurement strategy of both normal analytical peak scanning over a small mass range and also the one elaborated for recording an energy spectrum is schematically shown in Fig. 4. In normal operating mode (mass scanning) the computer sequentially sends small voltage steps through a digitial-to-analog converter to the instrument unit which controls the voltages on the electrostatic sector plates. The order of magnitude of these voltage steps is in the millivolt range. This electrostatic

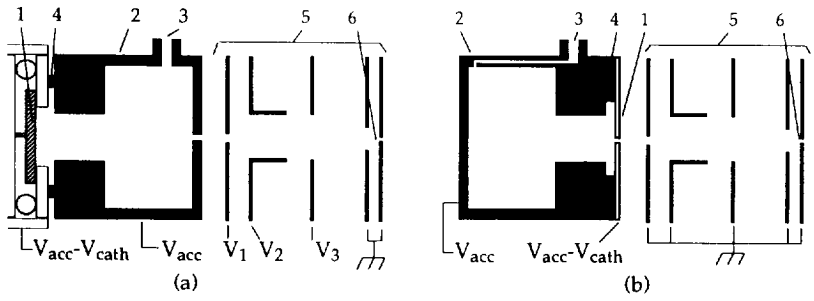

Fig. 5. Standard cell and focus stack configuration for the analysis of flat samples (a), and reversed configuration for the measurement of the energy distributions of ions bombarding the cathode (b); 1, cathode; 2, anode; 3, gas inlet; 4, insulator; 5, focus stack; 6, beam defining slit.

analyzer control unit then delivers an output voltage consisting of an offset voltage (y V) plus the voltage step sent by the computer to the instrument unit for the high voltage supply. Here this voltage is multiplied by a factor of one thousand (e.g. from 8.345 V to 8.345 kV). At the same time, it is used as a reference value for electronically altering the voltages on the electrostatic sector plates to keep the ratio V_{acc}/ϵ constant. The high voltage thus obtained is used as accelerating voltage and mass scanning (V_{acc}/ϵ = constant) is achieved.

The high voltage supply can, however, also be used independently to set a certain constant accelerating voltage. By redirecting the small voltage steps given by the computer directly into the high voltage supply unit, where they are multiplied and added to the offset potential which is set manually, energy scanning is obtained because now no variation in the voltage across the electostatic sector plates is induced. The minimum voltage step which the computer is capable of sending is 1 mV. After transformation this amounts to a 1 V accelerating voltage change, superimposed on a constant voltage of, for example, 5 kV. Choosing a slightly higher voltage step, e.g. 3 mV, and 300 scan points with the computer, it is clear that the accelerating voltage can be varied over a large range in a single energy scan (e.g. from 5000 to 5900 V). It should be mentioned that the total accelerating voltage at which ions with only thermal energy (0 eV on our energy scale) are transmitted is an instruumental constant. This value can thus be used as a calibration point for the energy axis of the spectra. Although this measurement strategy involves some modifications to the instrument, it allows use of the software designed for a normal mass scanning routine to acquire the energy spectra.

3.2. *Cell configuration*

In the normal analytical configuration of the VG9000 mass spectrometer the ions are sampled out of the NG region of the discharge plasma. To measure the energy distribution of ions impinging on the sample surface (cathode), a specific glow discharge cell had to be designed enabling the extraction of these ions into the mass spectrometer.

For the normal cell configuration, reference is made to Fig. 5(a). If the polarity of this cell is reversed and the exit slit plate can be made to function as the cathode of the GD system, a part of the ion flux bombarding the cathode surface can be sampled. The design of such a cell is presented in Fig. 5(b). Now the plate with the exit slit is electrically insulated from the rest of the cell which forms the anode of the system. The position of the gas inlet is instrumentally fixed; by providing a small channel in the anode body it was possible to introduce the gas at the back of the cell, so that the CDS is not too much influenced by a possible gas flow. The anode body was made from stainless steel. The exit slit is a 0.05×2 mm^2 opening in a 0.25 mm thick plate made from different materials (Al, Cu, Mo and Ta). Such a small slit size reduced the penetration of the extraction field considerably so that the CDS is only

disturbed to a minimal extent. The different cathode materials were all exposed to an argon discharge at different operating conditions. With molybdenum as cathode, neon was used as discharge gas. It was not possible to obtain an accurate knowledge of the pressure inside the cell: this was also the case for the analytical configuration. The pressure outside the cell in the vacuum housing is therefore used as reference. Exactly reproducing equal pressures when the cathode slits were changed, was not possible; hence the pressures mentioned in Section 4 should only be taken as an indication of the operating pressure inside the cell. Cryo-cooling is applied for all measurements.

In the analytical configuration the extracted positive ions are accelerated to 8 keV when they cross a focus stack of which the potential on the different plates is gradually reduced from 8 kV to ground potential. This focus unit can bring about energy selection by preferential focusing of ions of certain energy. To reduce this, only the first plate directly behind the discharge cell is used as acceleration electrode, the other plates being connected to ground potential. The small separation between this extraction electrode and the cell did not allow a 8 kV acceleration voltage; therefore a reduced value of 5 kV was selected. This implied, however, that the magnetic field strength and the electrostatic section voltage also had to be adjusted accordingly.

The final beam formation is done with a beam defining slit of fixed width (0.1 mm) placed at the end of the focus stack and adjustable in a direction perpendicular to the direction of the ion beam. Divergence of the extracted ion beam was inevitable, but this slit did not cause preferential energy selection: lateral displacement of the beam defining slit only induced a reduction in intensity without any appeciable difference in the shape of the energy distribution. Hence, the ion beam at this stage could be considered laterally homogeneous in energy. The voltage on the Einzel lens situated behind the focus stack was set to ground potential.

4. Results and Discussion

Energy spectra are recorded for different ionic species at three different pressure regimes and for each pressure three different discharge voltages (500, 750 and 1000 V) and thus also three different currents. Most theoretical models for GD systems assume the existence of only singly charged gas ions as positive charge carriers. It is, of course, not surprising that other ionic species which arrive at the cathode surface could also be detected, although for some at much lower intensities. The transport behaviour of these other ions in the CDS has not theoretically been treated in this work, but their energy distribution at the cathode may provide extra information regarding the processes occurring in the dark space. Reproducible results are obtained for the following ions: X^+, X_2^+, X^{2+}, M^+ and MX^+ where X denotes the gas used (argon and neon) and M the cathode material (Al, Cu, Mo and Ta). In what follows, the general outlook of the energy distributions of the different ions will be examined and then the effect of discharge parameters (pressure and voltage) will be investigated.

4.1. *General outlook of the energy distributions*

4.1.1. *Singly charged gas ions: Ar^+ and Ne^+.* In view of the theoretical model of which some results are presented in the previous section, which assumes only the existence of singly charged gas ions as positive charge carriers in the CDS, the experimental energy distribution of Ar^+ ions is of course the most significant. Fig. 6 presents this distribution for a discharge operating at 750 V and 3.4 mA; the energy axis is normalized to the energy corresponding to full discharge potential (750 eV). At first sight, at higher energies the experimental distribution resembles the one theoretically expected quite well (see Fig. 2(a)). However, starting from high energy, instead of a continuous increase towards zero energy, the signal intensity in the experimental distribution drops sharply at lower energies and shows, furthermore, a very large peak at negative energy. This depletion of low energy ions has also been observed by other authors [7, 9], and has, up to now, been explained by an energy discrimination effect: ions of low energy emerging from the discharge environment

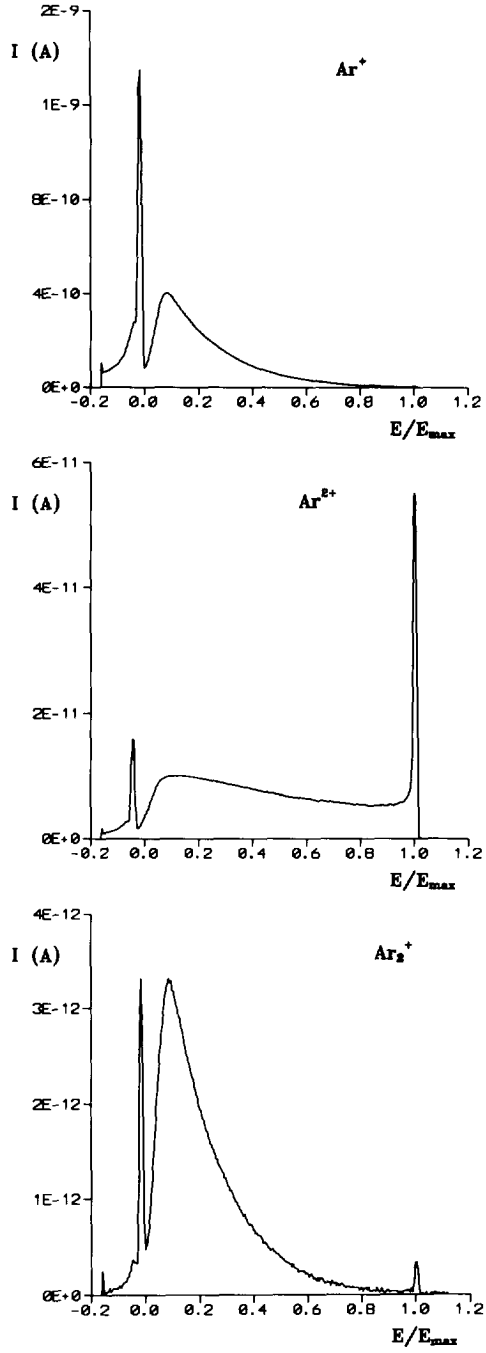

Fig. 6. Measured energy distribution of Ar^+, Ar^{2+} and Ar_2^+ ions at the cathode of a Cu/Ar glow discharge (750 V, 3.4 mA).

are presumed to be not well collimated by the accelerating field, thereby being lost in the further energy selection and detection process. However, one might intuitively expect the opposite. Ions with high energy are much more difficult to deflect from their initial direction of motion. So if some kind of preferential focusing should take place, it would probably lead to losses in the higher energy part of the spectrum. This statement can be backed up with the simulation of the ion trajectories of low and high energy ions in the specific configuration used here using a computer program [16], but will not be shown here. Another process which can account for the depletion (disappearance) of low energy ions might be ion-electron volume recombination. Close the cathode surface the energy gained by the electrons present in the dark space can

be low enough to promote recombination, but the cross section for this process can be considered too low [17].

Moreover, neither energy discrimination nor recombination offer any explanation for the large peak occurring at negative energy in the spectrum. Negative energy means in this case that the ions did not acquire the full accelerating potential, indicating that they must have been formed outside the discharge cell, somewhere in the accelerating field between the cell and the extraction electrode. The position of the peak (close to zero, at about −15 eV) suggests that these ions are created very near to the exit slit and its magnitude implies a formation process of high probability. Ionization in the accelerating zone can indeed take place if it is recognized that the vacuum conditions are far from perfect due to the gas flow out of the discharge cell. Numerous ionization mechanisms exist, but most of them can be regarded as being of low probability considering the specific configuration used here. Electron impact ionization requires the availability of an electron population with significant energy (typically around 100 eV) which is unlikely to be found in the accelerating zone. This leaves ionization induced by ion collisions: ion impact ionization and charge exchange. The cross section for ion impact ionization is at least one order of magnitude lower than that for charge exchange [14], so that charge exchange is probably the main process which can account for the ions observed at negative energy. This, however, has an important consequence. Because the energetic ions which induce charge exchange outside the cell are converted into fast neutrals, they are lost to the measuring process. Hence, charge exchange outside the cell will influence the energy distribution which is intended to be measured, the distribution of ions hitting the cathode after being accelerated across the dark space. Each ion which causes a collision in the accelerating zone will be removed from the original energy distribution; the newly created ion (wtih 0 eV initial energy) cannot pick up the full accelerating potential and will appear at negative energy (of which the actual value is indicative of the position where the charge exchange collision has taken place).

Although this hypothesis explains qualitatively the occurrence of the high peak at negative energy and at the same time suggests a loss process for the original distribution of ion energies at the cathode, it cannot quantitatively account for the heavy depletion of low energy ions observed in the energy spectrum. The cross section for charge exchange is, indeed, only moderately energy dependent [18]: in the energy range considered, all ions will cause charge exchange collisions outside the cell without too much difference in probability for ions of different energy. If the increased depletion of ions towards lower energy has to be explained by charge exchange, the cross section for this process would have to increase much more towards lower energy. A numerical example can illustrate this even more clearly. Starting from an arbitrary, theoretically calculated, ion flux energy distribution at the cathode, the loss in flux intensity, $\Delta J_i(E)$, due to charge exchange collisions outside the cell can be written as

$$\Delta J_i(E) = - N_g \Delta x \sigma_{ce}(E) J_{i,theor}(E)$$

with $J_{i,theor}(E)$ the theoretical flux distribution, $\sigma_{ce}(E)$ the cross section for charge exchange, N_g the gas density outside the cell and Δx the distance over which the collisions take place. The latter two are not known, but the value of their product can be estimated if it is assumed that the loss of the 0 eV flux, $\Delta J_i(E = 0)$ amounts to, for instance, 75% of the original flux, $J_{i,theor}(E = 0)$:

$$- \frac{\Delta J_i(E=0)}{J_{i,theor}(E=0)} = 0.75 = N_g \Delta x \sigma_{ce}(E=0)$$

At very low energy σ_{ce} is equal to 7.8×10^{-15} cm^2, which yields for $N_g \Delta x$ a value of 9.5×10^{13} cm^{-2}; this can be used to estimate the energy distribution at the cathode surface taking charge exchange outside the cell into account:

$$J_{i,ce}(E) = J_{i,theor}(E)(1 - N_g \Delta x \sigma_{ce}(E))$$

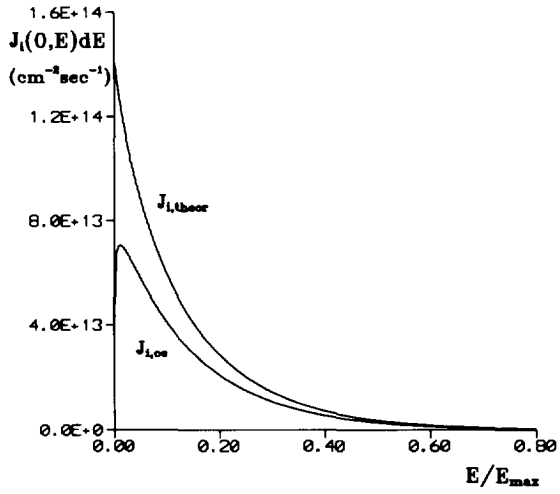

Fig. 7. Theoretical energy distribution for Ar^+ ions at the cathode ($J_{i,theor}$) and the calculated distribution obtained by taking into account charge exchange collisions outside the discharge cell ($J_{i,ce}$).

The result is shown in Fig. 7. The obtained distribution has a maximum very close to zero energy, and might give the impression that this reasoning can explain the observed depletion of ions in the experimental distribution. However, the total calculated flux loss due to charge exchange outside the cell (i.e. the sum over all energies), also has to correspond with the flux intensity observed at negative energy. But the obtained value is approximately 50 times too high compared to experiment and indicates that the strong depletion of low energy ions (assumed to amount to 75% at 0 eV) cannot be accounted for by charge exchange alone.

To summarize, it can be stated that the high peak at negative energy in the experimental distribution is, indeed, probably due to charge exchange collisions outside the cell, but that the reason for the large dip in the energy spectrum at low positive energies is still to be found. It is tempting to associate this with energy discrimination, but this explanation seems in contradiction with the fact that low energy ions are more easily collimated and therefore less likely to be lost in the mass spectrometer. Nonetheless, if it is assumed that charge exchange outside the cell affects the original distribution to only a minor extent (1–5%, estimated from the intensity of the observed peak at negative energy), the higher energy part of the spectrum can still be used to compare theory and experiment. The experimental distribution for the Ar^+ ions then at least confirms the important prediction that most of the ions arriving at the cathode have energies much lower than the discharge potential equivalent. The cathode is indeed bombarded by a large flux of low energy gas ions, as is theoretically expected. Further validation of the theoretical model follows when parameter changes are evaluated.

Essentially the same spectrum is obtained for singly charged neon ions, in the case of a neon discharge (see Fig. 8). It has to be noted that a neon discharge requires a much higher operating pressure than an argon discharge to achieve comparable current/voltage characteristics. The reason for this is the higher ionization potential of neon: the lower ionization efficiency in a neon discharge demands a (3 to 5 times) higher gas pressure to maintain a certain current at a given operating voltage. The energy distribution of Ne^+, however, does not reflect this higher pressure; only a small shift towards lower energies is observed. This means that the number of charge exchange collisions in the cathode dark space for both kinds of ion in their parent gases (Ne^+/Ne and Ar^+/Ar) is comparable. As has been previously discussed, the number of collisions is determined by the ratio of the dark space length to the mean free path for charge exchange, d_c/λ_{ce}. The mean free path length itself is determined by the

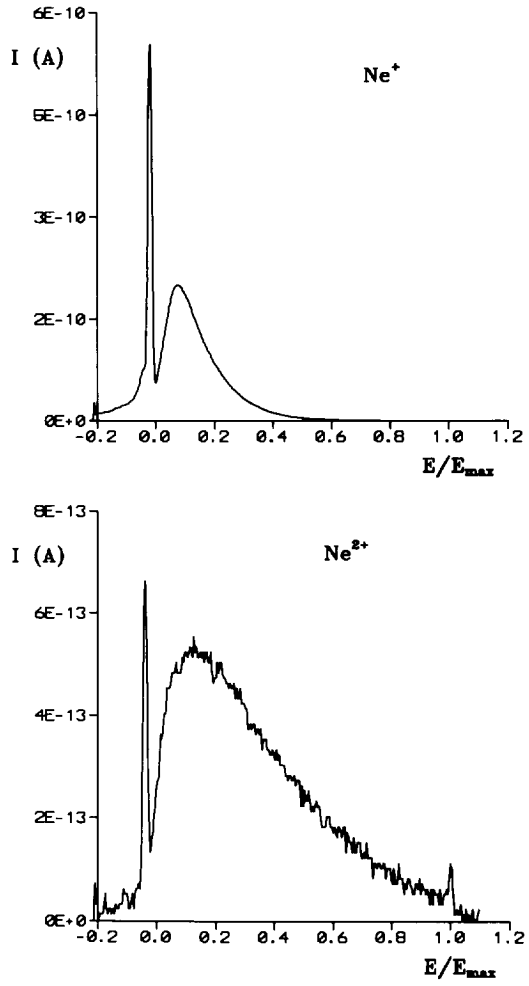

Fig. 8. Measured energy distribution of Ne^+ and Ne^{2+} ions at the cathode of a Cu/Ne glow discharge (750 V, 0.8 mA).

pressure and the cross section for charge exchange, which is not too different for the two gases ($\sigma_{ce}(Ne) = 0.6\sigma_{ce}(Ar)$). Hence, in order to have a comparable number of collisions in both cases, the higher pressure for the neon discharge implies a considerably thinner dark space.

4.1.2. *Doubly charged gas ions*: *Ar^{2+} and Ne^{2+}*. Fig. 6 illustrates the recorded energy spectrum for Ar^{2+} ions at the cathode of a glow discharge operating at 3.4 mA and 750 V. This spectrum is clearly different from the Ar^+ spectrum in that it exhibits a large peak at maximum energy. Again there is an apparent energy discrimination for low-energy ions ($<0.1\ E_{max}$) and a peak at negative energy. The energy distribution, including the depletion at very low energies, is similar to the one found by other works [7, 9]. The large peak at maximum energy indicates that a considerable fraction of the Ar^{2+} ions, formed in the negative glow or at least at the CDS/NG interface, has traversed the CDS without participating in any energy loss collision. There is no other explanation to account for ions with an energy equivalent to the full discharge potential. Some Ar^{2+} ions originating in the negative glow will lose energy by collisions on their way to the cathode and others will be formed in the dark space, both giving rise to the flux of ions at intermediate energies. The most probable mechanisms for these processes are as follows (f and s denote fast and slow, respectively):

	σ_{avg} (cm^2) [19–21]
$Ar_f^{2+} + Ar_s \rightarrow Ar_f + Ar_s^{2+}$	$7–9 \times 10^{-16}$
$Ar^{2+} + Ar \rightarrow Ar^+ + Ar^+$	$2–3 \times 10^{-16}$
$Ar + e^- \rightarrow Ar^{2+} + 3e^-$	$1–3 \times 10^{-17}$
$Ar^+ + e^- \rightarrow Ar^{2+} + 2e^-$	–

The first two reactions are charge exchange collisions, whereby it is noted that the (average) cross section for the symmetrical reaction is larger than for the asymmetrical one, even though this implies the simultaneous exchange of two electrons. Although both reactions are energy loss processes, the first one yields a slow Ar^{2+} ion which can still be present at the cathode surface, but the second one removes the Ar^{2+} ion out of the distribution. The two electron impact ionization reactions which create doubly charged gas ions are generally of less importance. Of these, direct twofold ionization can be regarded more probable than ionization of singly charged argon ions, giving the large difference in density between Ar^+ and Ar. It is difficult (or even impossible) to distinguish directly from the energy spectrum whether the Ar^{2+} ions of intermediate energies are created by charge exchange or ionization processes. The values of the cross sections, however, indicate that charge exchange, taking place somewhere in the dark space, will have more influence on the energy of the Ar^{2+} ions at the cathode surface.

Compared to the Ar^+ spectrum, the difference in cross section for symmetrical charge exchange ($Ar_f^+ + Ar_s \rightarrow Ar_f + Ar_s^+$, $\sigma_{ce} = 2–5 \times 10^{-15}$ cm^2 [18]) is the main reason for the different outlook of the energy distribution of Ar^{2+}, because the operating conditions in both cases are identical and thus also the length of the CDS. The intensity of the peak at negative energy relative to the rest of the spectrum for Ar^{2+} is also much lower than observed for Ar^+ and can be explained by the same fact. This supports the assumption that these peaks are due to charge exchange collisions outside the discharge cell.

In the energy spectrum of Ne^{2+} ions, obtained using neon as discharge gas, the peak at maximum energy is much lower, and in general a higher intensity is obtained at lower energies (see Fig. 8). All these features can be attributed to the higher operating pressure for a neon discharge (necessary to maintain comparable current/voltage values).

4.1.3. *Molecular ions: Ar_2^+, Ne_2^+ and $CuAr^+$.* Apart from a small peak at maximum energy and a lower intensity of the negative energy peak, the spectrum for Ar_2^+ ions (Fig. 6), is remarkably similar to that of Ar^+. In fact, if the positive energy parts of both spectra are normalized, so that they correspond to one ion in the cathode dark space, it can be shown that these distributions coincide almost completely. A possible explanation for this observation is the formation of the Ar_2^+ molecular ions according to the associative reaction (cationization of Ar by Ar^+)

$$Ar^+ + Ar \rightarrow Ar_2^+ \qquad (1)$$

with the fulfilment of certain additional conditions to obtain identical energy distributions for both Ar^+ and Ar_2^+ ions at the cathode surface. The most stringent of these is the necessity that all measured Ar_2^+ ions have to be formed within one mean free path in front of the exit slit of the discharge cell. Secondly, reaction (1) should not be energy dependent, nor endo- or exothermic (at least not measurably). Thirdly, it must be a process of very high cross section because the relative absolute intensities of the Ar^+ and Ar_2^+ spectra indicate an association efficiency of around 1%. The first two conditions must be satisfied otherwise one of the two distributions would be shifted in energy compared to the other.

The first condition requires that all Ar_2^+ ions formed further away from the cathode

have to be lost by other collision processes on their way to the cathode. The most probable is the dissociative reaction

$$Ar_2^+ + Ar \rightarrow Ar^+ + 2Ar \tag{2}$$

which is believed to be much more significant than the charge exchange reaction

$$Ar_2^+ + Ar \rightarrow Ar + Ar_2^+ \tag{3}$$

involving the exchange of an Ar^+ ion. The relatively low intensity of the peak at negative energy for Ar_2^+ compared to the rest of the spectrum indeed suggests that reaction (2) plays a more important role than charge exchange.

In addition, all these assumptions must not be contradictory with the occurrence of the small peak at maximum energy. As for Ar^{2+}, this peak can only be due to ions formed in the negative glow which traverse the dark space without making any collision. It is known from the normal operating conditions that the Ar_2^+/Ar^+ ratio in the negative glow is quite high (typically about $2\text{–}5 \times 10^{-2}$). Because the rest of the distribution is believed to be governed by the associative reaction (1) at or near the cathode, the small peak at maximum energy indeed indicates that the dissociative loss reaction (2) is of high probability. Otherwise the peak at maximum energy would be higher and/or (if resonance charge exchange were important) the distribution of Ar_2^+ would have to be considerably different from that of Ar^+.

To summarize:

(i) Ar_2^+ ions hitting the cathode surface are most probably formed by an associative reaction of Ar^+ with Ar very close to the surface (within one mean free path).

(ii) The small peak at maximum energy corresponds to ions formed in the negative glow; the abundance of Ar_2^+ ions at the interface must be much higher. Most of the Ar_2^+ ions in the CDS, either formed by association of Ar^+ with Ar at positions further than one mean free path length away from the cathode or those originating at the interface, are lost through a dissociation collision.

For all discharge conditions investigated and cathode materials used, the normalized energy distributions for Ar^+ and Ar_2^+ coincide and the same results are obtained when neon is used as discharge gas (Ne^+, Ne_2^+). The interpretation of the Ar_2^+ spectrum given here involves the (most unlikely) simultaneous fulfillment of several conditions, but no other reasonable explanation could be found.

When using copper as the cathode, the argide $CuAr^+$ could also be detected at the cathode surface. The energy spectrum is shown in Fig. 9, and at first sight is comparable to the Ar^{2+} spectrum but no peak is observed at negative energy. A possible energy loss reaction for $CuAr^+$ ions originating at the negative glow interface is the ion-interchange reaction

$$CuAr_a^+ + Ar_b \rightarrow Ar_a + CuAr_b^+ \tag{4}$$

where the subscripts a and b are used for distinction purposes. It is difficult to estimate the amount of energy loss for the $CuAr_a^+$ ion which accompanies this reaction. The cross section of this process will probably be low, but nevertheless it will determine the $CuAr^+$ energy distribution at the cathode, together with the following association reactions in the dark space:

$$Cu^+ + Ar \rightarrow CuAr^+ \tag{5}$$

$$Cu + Ar^+ \rightarrow CuAr^+ \tag{6}$$

Reaction (5) benefits from the high neutral gas atom density compared to the copper atom density. Both association reactions can, however, be assumed to be even less important than the ion-interchange reaction.

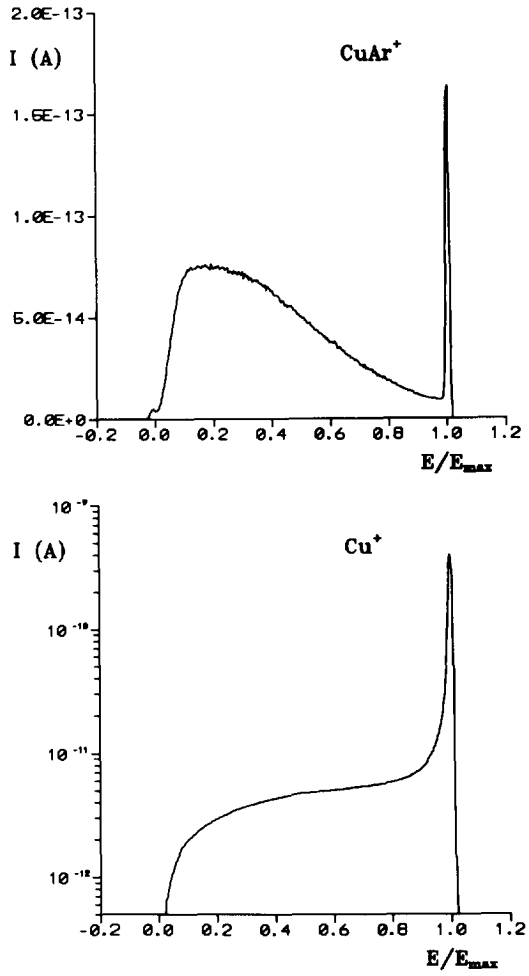

Fig. 9. Measured energy distribution of $CuAr^+$ and Cu^+ ions at the cathode of a Cu/Ar glow discharge (750 V, 3.4 mA).

More probable are the dissociation collisions

$$CuAr^+ + Ar \rightarrow Cu^+ + 2Ar$$

$$CuAr^+ + Ar \rightarrow Cu + Ar^+ + Ar$$

which remove the $CuAr^+$ from the measured energy distribution. The ratio $CuAr^+/Cu^+$ in the negative glow region is known from normal mass spectrometric operation to be very high (10^{-2} to 10^{-1}) compared to the argides formed with other metals. If this is compared to the $CuAr^+/Cu^+$ ratio at the cathode surface (10^{-4} to 10^{-3}), it must be concluded that dissociation is indeed decisive in the fate of the $CuAr^+$ molecular ion. A finite amount of $CuAr^+$ ions will, however, survive the acceleration process across the dark space for which reaction (4) then applies.

4.1.4. *Singly charged cathode ions*: M^+. Although not immediately expected, the experiments showed that the cathode is also bombarded with a significant flux of ions of its own material. The energy distribution of Cu^+ ions at the cathode surface (made of copper) in an argon discharge is shown in Fig. 9 (note the logarithmic scale). In strong contrast with the Ar^+ spectrum, this distribution peaks sharply at maximum energy; very few ions with intermediate energies are detected. The total Cu^+ flux at the cathode is about 20% of the Ar^+ flux. Most, if not all, of the Cu^+ ions arriving at the cathode are formed in the negative glow and reach the cathode without energy

loss collisions. This spectrum forms the indirect evidence that ionization of sputtered material is negligible in the CDS, at least at these typical operating conditions.

The low ion intensity at intermediate energies can either be the result of slowing down collisions of ions originating in the negative glow, or ionization in the CDS of sputtered cathode atoms. The possible charge exchange collisions for a Cu^+ ion starting at the CDS/NG interface are

$$Cu_f^+ + Ar_s \rightarrow Cu_f + Ar_s^+ \tag{7}$$

$$Cu_f^+ + Cu_s \rightarrow Cu_f + Cu_s^+ \tag{8}$$

where f and s denote fast and slow, respectively. Exact values are not known, but the cross section for symmetrical charge exchange (reaction (8)) will be much higher than for the asymmetrical case (reaction (7)). The latter may, however, still be more probable due to the much higher neutral gas atom density compared to the sputtered atom density. The importance of the asymmetrical reaction is hard to estimate because it removes Cu^+ ions from the measured distribution. The cathode ions with intermediate energies have then to be formed by reaction (8) or by direct ionization. Ionization by electron impact is unlikely but, for example, Penning ionization in the dark space cannot be ruled out completely.

Again, there is no significant difference in the shape of the energy distribution of cathode ions when neon is used as discharge gas, nor when other cathode materials are chosen. With neon, a shift towards lower energies is noticeable and the peak at maximum energy is smaller (not shown here). Remembering the higher operating pressure for a neon discharge, this suggests that asymmetrical charge exchange becomes more important at higher pressures.

The total flux of cathode ions compared to the singly charged argon ions at the cathode surface is anything but negligible. Hence, the influence of self-sputtering, i.e. sputtering of cathode material by ions of its own material, should be taken into account because the cathode ions, although outnumbered by the argon ions, have a much higher energy when they reach the cathode. To estimate the importance of this effect, the sputter yields for these two kinds of ions as a function of energy were calculated using an empirical formula for the energy dependence of the sputter yield [22] and starting from the normalized measured energy distributions for both ions. Because the energy distribution of Ar^+ ions may be influenced by measurement artifacts at low energy, it was deemed preferable to extrapolate the experimental Ar^+ distribution at lower energies using the higher energy part of the spectrum. The normalized spectra and the results of the sputter yield calculations are shown in Fig. 10. Integrating over all energies gives the total sputter yield for both types of ions ($Y_{tot,Ar} = 0.83$; $Y_{tot,\,Cu} = 3.17$). The unexpectedly high value for the total sputter yield due to cathode ions results from the combination of an increasing intensity of copper ions towards high energy, and a higher sputter yield for bombarding ions of high energy and mass. Incorporating the measured total Ar^+- and Cu^+-fluxes towards the cathode, it can be estimated that the sputter rate of the copper cathode is for about 40% due to ions of its own material. The same method was applied to calculate the total sputter yield due to argon and cathode ions for other cathode materials. For a 1000 V discharge, at a (probably) comparable pressure to that used for copper, the results are summarized in Table 1. The difference in discharge current (at constant voltage and pressure) for the different materials can mainly be attributed to a difference in secondary electron emission coefficient. For all investigated cathode materials, the total sputter yield due to argon ions is much lower than the one due to cathode ions (factor 2 to 8). The interelement difference in Y_M^+ is not so large (except for copper), but the relative importance of self-sputtering shows a considerable variation with cathode material. This can be explained by the large difference in the M^+/Ar^+ flux ratio at the cathode, which is the smallest in the case of molybdenum.

In the literature, some workers have reported that the cathode is indeed bombarded by cathode ions, but the significance of self-sputtering to the atomization in a glow

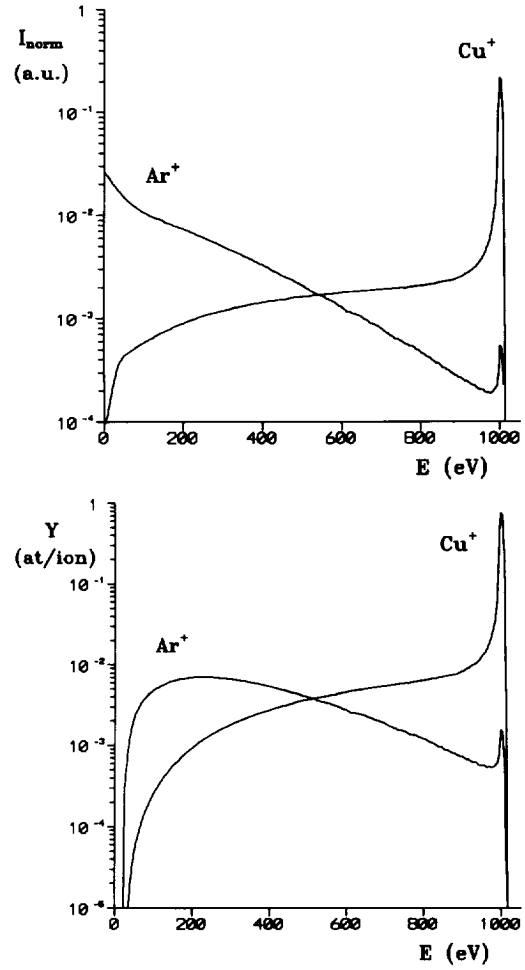

Fig. 10. Normalized measured energy distributions of Ar^+ and Cu^+ ions at the cathode of a Cu/Ar glow discharge (top) and the corresponding sputter yield for both elements (bottom).

Table 1. Discharge current, total ion current at the cathode for Ar^+ and M^+, total sputter yield for $Ar^+$and M^+, and relative importance of self-sputtering for different cathode materials

	I_{disch} (mA)	I_{Ar^+} ($\times 10^{-8}$ A)	I_{M^+} ($\times 10^{-9}$ A)	I_{M^+}/I_{Ar^+}	Y_{Ar^+} (at/ion)*	Y_{M^+} (at/ion)*	% Self-sputtering*
Al	9.0	6.84	12.7	0.186	0.64	1.25	26
Cu	4.8	2.32	4.36	0.188	0.83	3.17	42
Mo	5.0	5.53	0.84	0.015	0.27	1.19	6
Ta	1.8	0.72	0.54	0.074	0.15	1.15	36

*Calculated, see text.

discharge has never been quantified. So it is not easy to back up the unexpectedly higher values obtained here with literature data. In Ref. [10] the intensity of the Cu^+ flux at a copper cathode can be prudently estimated from a graph to be less than 1% of the Ar^+ flux intensity, and this, in spite of the fact that the discharge conditions were comparable to the ones used in the present work (1360 V, 3.10 mA and 20 Pa). Other data could not be found.

The evaluation presented here neglects the contribution of bombardment by fast argon atoms, created by charge exchange collisions in the dark space, to the sputtering

process. It has been demonstrated theoretically that these species can form a major contribution to the sputter yield (up to 80% [12, 13]). To confirm this experimentally, it is necessary to elaborate a procedure to measure the neutral flux (as a function of energy) bombarding the cathode. In order to apply mass spectrometry for this purpose, a means for ionization of the fast neutrals is obligatory. If such a type of experiment can be performed in the future, it would allow assessment of the importance of fast atom bombardment in the atomization process of a glow discharge.

Although perhaps not directly anticipated, the high intensity of cathode ions at the cathode surface might also have an analytical application. In this particular experimental configuration, without paying any attention to proper ion beam focusing, the cathode (matrix) ion current amounts to about 10^{-10} to 10^{-9} A for ions with an energy equivalent to full discharge potential. This does not differ significantly from the attainable matrix ion intensity in normal operating conditions. At the same time, the intensity of Ar^+ ions with this energy is almost three orders of magnitude lower. Although other ionic species (e.g. $CuAr^+$, Fig. 9) may peak at maximum energy, their intensity at the cathode surface is, in general, orders of magnitude lower than obtained in normal operating conditions, i.e. for negative glow ion sampling. Hence, mass spectral interferences can be avoided by sampling ions at the cathode end of a glow discharge combined with proper energy selection. This would be especially beneficial in quadrupole based GDMS. However, with a quadrupole filter proper mass separation is only achievable for ions with very low initial energy, so that a decelerating lens system would be necessary. A second instrumental difficulty, which perhaps would not be so easy to overcome, is that samples have to be shaped in such way that ions can be extracted from the cathode end of the discharge.

4.2. *The effect of parameter changes*

With copper as cathode material and argon as discharge gas, the effect of the discharge conditions on the measured energy distributions of the different ions will now be discussed. The distributions are recorded for three different pressures at constant voltage and for three different voltages at constant pressure. The discharge current is in each case also different, but by normalizing the obtained distributions its influence can be excluded.

It is mentioned that the actual pressure inside the discharge cell is not known. The pressure values indicated on the figures below correspond to the pressure measured outside the cell and can only be used as a relative measure of the operating discharge pressure without any absolute meaning. Only results obtained when copper is used as the cathode are shown, but for all other cathode materials comparable results are obtained for all ion types. The same applies for the equivalent gas ionic species when neon is used as discharge gas instead of argon.

4.2.1. *Singly charged gas ions: Ar^+ and Ne^+.* For Ar^+ ions, the results are shown in Fig. 11(a) and 11(b). At constant discharge voltage (750 V) (Fig. 11(a)) the energy distribution shifts to higher energies for higher discharge pressures. At first sight, this might seem odd, because one would expect an increasing number of charge exchange collisions with increasing pressure, and therefore more energy loss. However, as demonstrated earlier for the theoretical distributions, the effect of a changing dark space length with pressure has to be taken into account. The number of charge exchange collisions, and thus the energy of the Ar^+ ions at the cathode, is determined by both the gas number density and the total distance which an ion has to travel from the negative glow interface. If both quantities are influenced by the pressure to the same (relative) extent, then the number of charge exchange collisions per ion, at constant voltage, does not vary greatly with pressure and hence will yield comparable normalized energy distributions. This is more or less observed for the calculated distributions which at constant voltage almost coincided for the three pressures investigated (50, 75 and 100 Pa, see Fig. 3(a)). The energy shift in the experimental distribution towards higher energy with increasing pressure is, however, more pronounced and shows that the dark space length must change much more with

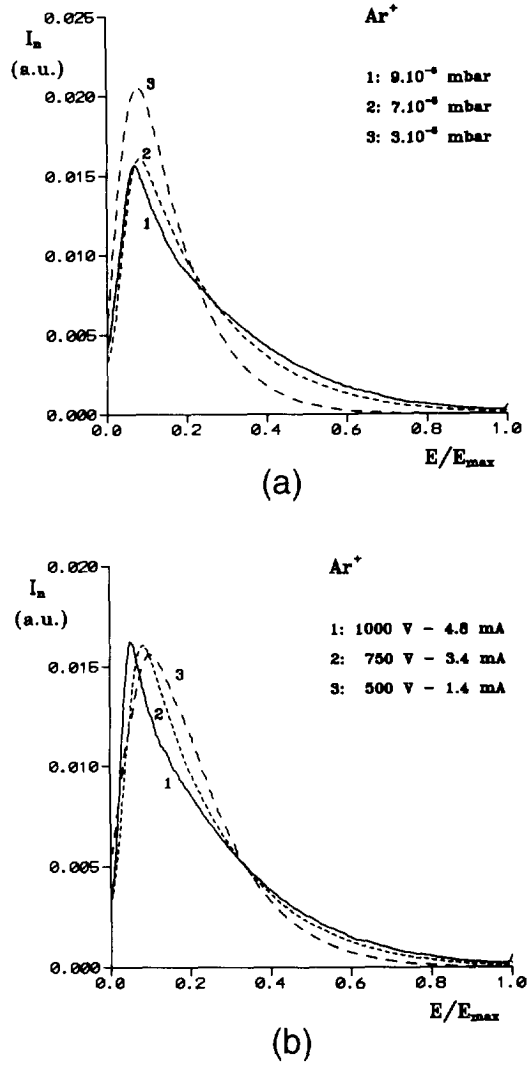

Fig. 11. Measured energy distributions for Ar^+ ions at the cathode of a Cu/Ar glow discharge at constant voltage (1000 V) for three different pressures (a), and at constant pressure for three different voltages (b).

pressure than the number density of the gas ions (which is linearly proportional to the pressure). Up to now the only satisfactory explanation for this apparent discrepancy between theory and experiment might be the possible difference in pressure between experiment and theory. The experimental pressures are not known, but the current/voltage characteristics indicate that lower pressures are applied for the experiments than for the theoretical calculations. It can be possible that the change in the length of the dark space for a certain pressure change is much larger at a low pressure than at high pressure (or in other terms, $\Delta d_c/\Delta p$ is a function of p).

At constant pressure (Fig. 11(b)), the experimental flux energy distributions for Ar^+ ions for different discharge voltages compare quite well with theory (see Fig. 3(b)) and reflect also the change in dark space length. At higher voltages the dark space is compressed, decreasing the probability for collisions and hence shifting the energy distributions slightly to higher energies. Comparing Figs. 11(a) and 11(b), a voltage change of 250 V seems to induce a smaller change in d_c/λ_{ce} than the applied pressure variation, but it is difficult to estimate which of the two parameters will have the largest influence because the operating pressure is not known. It is noted that all the low energy maxima in Fig. 11 occur at the same absolute energy, which might

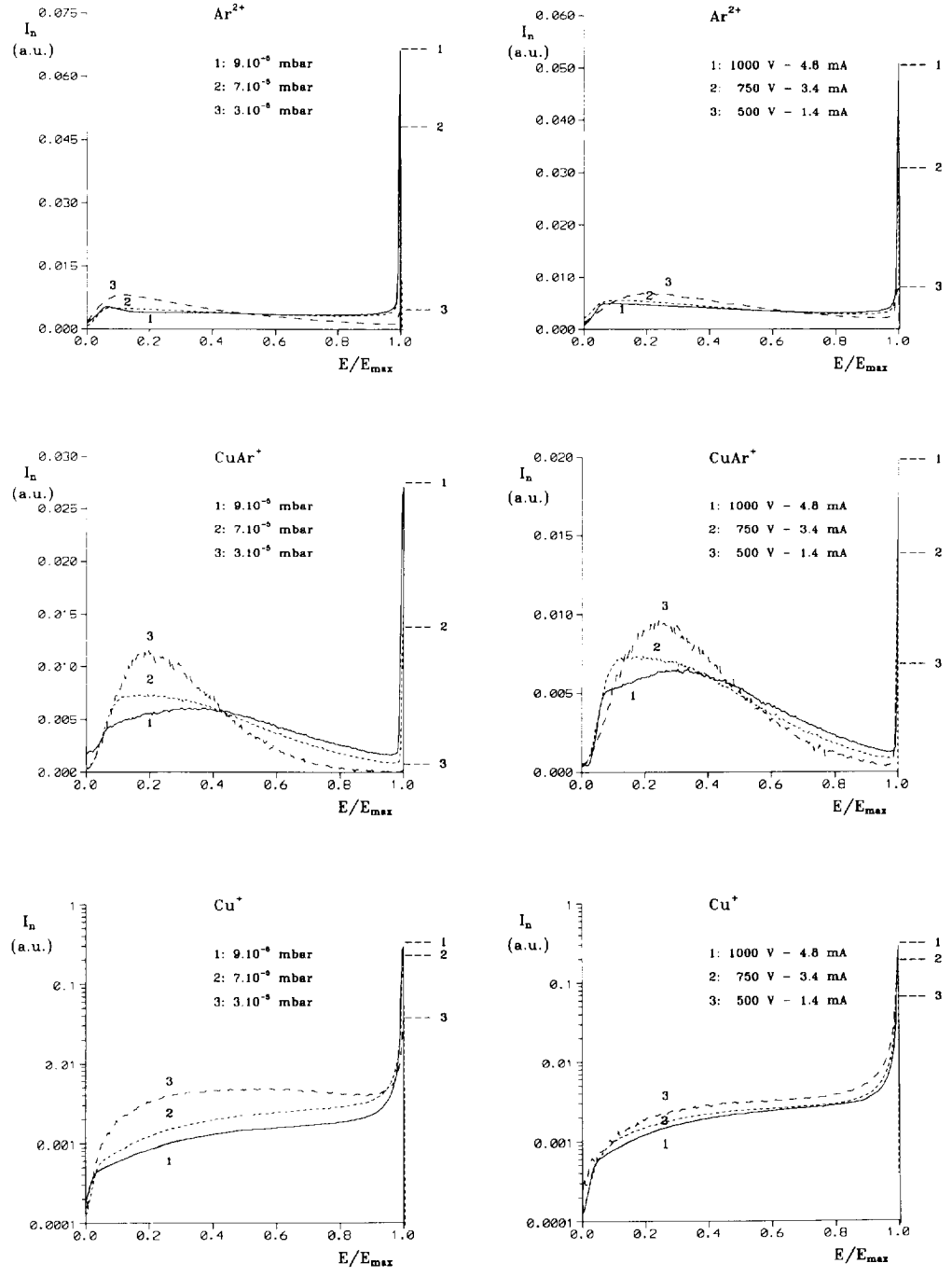

Fig. 12. Measured energy distributions for Ar^{2+}, $CuAr^{+}$ and Cu^{+} ions at the cathode of a Cu/Ar glow discharge at constant voltage (1000 V) for three different pressures (spectra on the left), and at constant pressure for three different voltages (spectra on the right).

indicate that the depletion of low energy ions is caused by an energy discrimination effect rather than by a phenomenon connected to a process in the dark space itself.

4.2.2. *Other ions.* The influence of the discharge parameters on the energy distributions is the same for all other detected ions. In Fig. 12 the results are shown for Ar^{2+}, $CuAr^{+}$ and Cu^{+} obtained at constant voltage (for different pressures; spectra on the left) and constant pressure (for different voltages; spectra on the right). In all distributions, the effect of a changing dark space length can be observed. At constant voltage, the dark space length varies more with pressure than the gas number density,

as is also found for Ar^+. The peak occurring at maximum energy becomes smaller when the pressure is decreased, and sometimes even vanishes for the lowest pressure. At constant pressure, the change in dark space length is less pronounced, but still induces a significant shift in energy. Although it is impossible to distinguish between ions formed in the negative glow and those formed in the dark space, it is hard to imagine that, in the pressure regime investigated, the ionization efficiency in the negative glow drops with increasing pressure, either for electron impact or Penning ionization. This should be the case when explaining the higher abundance of intermediate energy ions by ionization in the dark space. From the distributions for Cu^+, it can be seen that the importance of self-sputtering might be influenced by the operating conditions. It has to be noted, however, that the shifts in the energy distributions for gas ions and cathode ions induced by parameter changes, are in the same direction. Also, the relative total ion flux at the cathode M^+/X^+ will not vary greatly with the operating conditions, so that no important differences in the relative amount of self-sputtering are expected.

5. CONCLUSION

Gas ion motion in the CDS of a glow discharge is largely collision dominated, limiting and spreading out the energy of the gas ions when they reach the cathode. The theoretically expected variation in the ion energy distribution at the cathode when the discharge conditions are altered, is qualitatively backed up by experiment.

The number of charge exchange collisions with neutral gas atoms, either symmetrical or asymmetrical, determines the energy distributions of all kinds of ions at the cathode (ionization in the dark space is believed to be of minor importance). This number is influenced by the mean free path (determined by the pressure) and the length of the dark space. Variation of the discharge parameters has illustrated that the ratio of both quantities is not constant; the length of the dark space varies more with pressure than the number density of gas atoms.

The cathode is bombarded by a significant flux of ions of its own material. If sputtering by fast atom bombardment is excluded, the sputtered atom flux liberated from the cathode is for a considerable part (6–40% for the materials investigated; for discharge conditions comparable to those used in analytical applications) due to self sputtering. However, in view of the theoretically expected high flux of fast neutrals at the cathode, it seems worthwhile to develop a suitable experiment to evaluate the flux energy distribution of these fast atoms.

Acknowledgements—This research is sponsored by the Science Policy Programming Services (DPWB) of the Prime Minister's office through IUAP-III (conv. 49). A. BOGAERTS is indebted to the National Science Foundation (NFWO) for financial support.

REFERENCES

[1] J.A. C. Broekaert, in R. K. Marcus (Ed.), *Glow Discharge Spectroscopies*, Plenum Press, New York (1993).
[2] W. W. Harrison, in F. Adams, R.Gijbels and R. Van Grieken (Eds.), *Inorganic Mass Spectrometry*, John Wiley, New York (1988).
[3] R. K. Marcus, *J. Anal. Atom. Spectrom.* **8**, 935 (1993).
[4] N. P. Ferreira and H. G. C. Human, *Spectrochim. Acta* **36B**, 215 (1981).
[5] M. van Straaten, R. Gijbels and A. Vertes, *Anal. Chem.* **64**, 1855 (1992).
[6] J. A. Valles-Abarca and A. Gras-Marti, *J. Appl. Phys.* **55**, 1370 (1984).
[7] W. D. Davis and T. A. Vanderslice, *Phys. Rev.* **131**, 219 (1963).
[8] A. V. Bondarenko and M. A. Lebedev, *Sov. Phys.–Tech. Phys.* **12**, 774 (1967).
[9] A. V. Bondarenko, *Sov. Phys.–Tech. Phys.* **18**, 515 (1973).
[10] H. J. Denk, *Ph.D. Thesis*, University of Düsseldorf (1975).
[11] I. Abril, *Comp. Phys. Comm.* **51**, 413 (1988).
[12] M. van Straaten, *Ph.D. Thesis*, University of Antwerp (1993).
[13] A. Bogaerts, M. van Straaten and R. Gijbels, *Spectrohim. Acta B*, submitted.
[14] B. Chapman, *Glow Discharge Processes*, John Wiley, New York (1980).

[15] G. Francis, in S. Flügge (Ed.), *Encyclopedia of Physics*, Vol. 22, Springer-Verlag, Berlin (1956).
[16] D. Dahl and J. Delmore, *SIMION PC/PS2 Users Manual Version 4.0*, ECG-CS-7233 Rev. 2 (1988).
[17] J. B. Hasted, *Physics of Atomic Collisions*, Butterworth, London (1972).
[18] R. S. Robinson, *J. Vac. Sci. Technol.* **16**, 185 (1979).
[19] J. W. McGowan and L. Kerwin, *Can. J. Phys.* **45**, 1451 (1967).
[20] J. B. Hasted and M. Hussain, *Proc. Phys. Soc.* **83**, 911 (1964).
[21] W. Bleakney, *Phys. Rev.* **36**, 1303 (1930).
[22] Y. Yamamura, N. Matsunami and N. Itoh, *Radiat. Eff.* **71**, 65 (1983).